5th ECPMG Delft · 2024

Proceedings of the 5th ECPMG 2024
5th European Conference on Physical Modelling in Geotechnics
2-4 October 2024, Delft, the Netherlands

Viscous effects on granular debris flows

H.M. Nichols
University of Sheffield, Sheffield, UK, hmnichols1@sheffield.ac.uk

E.T. Bowman
University of Sheffield, Sheffield, UK, e.bowman@sheffield.ac.uk

ABSTRACT: Debris flows are saturated mass movements of granular material, consisting of various grain sizes, that travel at high speeds down slope. Fine grains, such as clay particles, are assumed to be constantly suspended by the interstitial fluid due to small settling velocities and continuous flow shearing. This process creates a viscous liquid with a non-Newtonian shear-thinning rheology. However, the effects of these attributes on the severity of overall flow behaviour and subsequent response to mitigation structures has divided the current literature. This leaves uncertainty surrounding suitable modelling of the critical design scenario. To target this, the study presented uses a viscometer to verify the shear-thinning nature of a kaolin clay suspension and a small scale flume to physically simulate non-viscous and viscous granular debris flows. Both unobstructed and slit barrier mitigated tests show the viscous flows to increase system energy retainment and therefore, increase flow mobility.

1 INTRODUCTION

Debris flows have high kinetic energies, with frictional losses occurring during particle and flow-channel contacts, collisions and interaction of the solid and fluid phases (Iverson 1997). As flow travels downslope grains move relative to each other in processes of dilation and contraction, leading to particle size sorting and segregation of the two phases (Coussot & Ancey 1999, Bowman & Sanvitale 2009, Turnbull, Bowman & McElwaine 2014, Kaitna et. al. 2016, Zhao et. al. 2024). The interstitial fluid has been observed to lubricate grains, reducing friction and increasing flow mobility with higher water content when minimal suction occurs as flow dilates (Iverson 1997, de Haas et. al 2015, Nguyen, Kang & Kim 2018, Zhao et. al. 2024). As climate change continues to alter weather patterns, this heavy rainfall triggered natural hazard is likely to occur both more regularly and at higher severities as more water may be contained in the flow (Turnbull, Bowman & McElwaine 2014). This may create an increasing risk for nearby populations and supporting infrastructure, such as on the A83 in Scotland, where debris flows regularly occur, as they would have higher velocities and longer runouts (Winter 2019, de Haas et. al. 2015).

Fine particles are commonly considered as part of the fluid phase, increasing the water viscosity as solids are in constant suspension (Iverson 1997). Rheological studies of kaolin suspensions consistently return a shear-thinning behaviour. Kaolin usually possesses a ‘house of cards’ arrangement of particles, created by surface electrostatic charge interaction (van Olphen 1977). The shear thinning is attributed to the faster deflocculation and dispersion of these clay particles than can be reformed into the usual house of cards structure (Michaels & Bolger 1962, Kameda & Morisaki 2022). The consequences of this behaviour on debris flow macro scale properties are unclear. Arguments have been made in favour of either an increased grain lubrication or overall higher frictional resistances. For example, physical model studies considering fines variation produced higher mobilities in de Haas et. al.’s (2015) flume study and lower mobilities in flume tests by Zhou et. al. (2019a) and centrifuge tests by Cabrera et. al. (2018), reflecting the complexity in modelling of fines in debris flows. To reduce this modelling uncertainty, most studies remove or reduce levels of clays particle sizes from the particle size distribution (PSD), use a dry flow or use a Newtonian viscous fluid additive, such as glycerol (e.g. Choi et. al. 2016, Hu et. al. 2020). However, this has left the understanding of the effect of viscosity and colloidal suspension behaviour on coarse grain motion unclear on a macro scale.

Debris flows are often mitigated against using a series of hard engineering structures, such as flexible or slit barriers and check dams, to retain flow (VanDine 2022). Slit barriers are designed to reduce flow velocity while utilising grain frictional contact via arching between larger particles, aiding flow retainment and allowing drainage of the interstitial fluid (Choi et. al. 2016, Zhou et. al. 2019). Current experimental tests have found optimal slit ratios, slit

gap (b) : maximum particle diameter (d_{max}), to be in the range of 2.3-3.6 (Zhou et. al. 2019, Hu et.al. 2020). This is lower than the ratio of 2.0 consistently used in industry settings (Choi et. al. 2016, Zhou et. al. 2019). However, most studies have made a simplification compromise for flow viscosity.

To study the influence of viscosity at a constriction, this paper describes use of a 5 % replacement of a monodisperse coarse grained sample mass with a kaolin clay. Slit barrier ratios selected are the upper (3.6) and lower (2.3) bounds of the ranges presented as optimal in existing studies.

2 METHODS

2.1 Kaolin suspension experimental testing

An elcometer® 2300RV (L) Viscometer without temperature gauge was used with TL5 and TL6 spindle (bulb) attachments to measure the dynamic viscosity of kaolin suspensions at increasing rotations per minute (rpm). Measurements were taken at each viscometer rpm setting in the range of 5 rpm to 200 rpm. The higher precision TL5 sensor of resolution 0.1 mPa*s was used for all test data, shown in Figure 1, with TL6 used for calibration purposes only (elcometer® 2007).

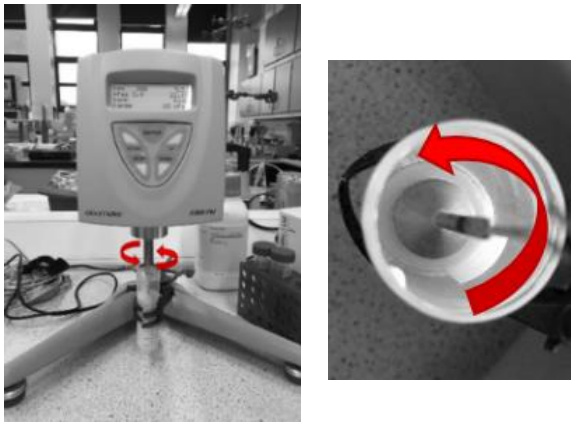

Figure 1. Viscometer equipment setup and loaded sample..

Each specimen was shaken, loaded onto the clamp system and the spindle slowly lowered into the suspension until approximately 5 mm of fluid was above the bulb. Once correctly positioned away from test tube side walls with no bubbles visible on the fluid surface, the spindle was allowed to rotate starting at 5 rpm and increasing to 200 rpm over the test duration. The dynamic viscosity and percentage of the sample engaged were recorded for each rpm in all three trials for both volume sizes. Measurements were recorded after 10 s and the output value stabilised. Rotations per minute were converted into shear rates using standard equipment factor 1.32 for the TL5 bulb with 8 cm^3 volume, as the proportion of water to kaolin used remained constant across different sample sizes (elcometer® 2007).

Table 1 shows the composition of the two sample volumes prepared, containing water with powdered kaolin stirred into suspension. The proportion added was 5 % of the water mass and specific gravity of kaolin was taken to be 2.65.

Table 1. Kaolin suspensions compositions.

Sample Name	Water Mass (g)	5% Water Mass (g)	Kaolin Mass (g)
KS_20	20	1	2.65
KS_30	30	1.5	3.98

2.2 Granular debris flow modelling

The small scale flume used here is 100 mm wide, confined by Perspex walls, and consists of two channel segments as shown in Figures 2 and 3. The upper section is inclined at 30 ° and has a roughened aluminium base which is instrumented with two load cells and an over-channel ultrasound to record total basal stresses and flow heights respectively at sampling rates of 36 kHz. Tests were recorded using a high speed camera of model 8000 Miro310 Phantom with an AF 1.4D Nikon Lense. The camera was positioned at either the instrumented channel section or at barrier location depending on the test conducted with images postprocessed, when possible, using in-house PIV MatLab code as used by Zhao et. al. (2024).

Figure 2. Flume apparatus photograph & diagram of slit barrier channel location.

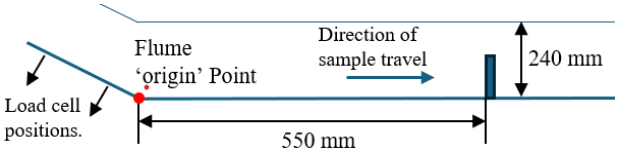

Figure 3. General arrangement of slit barrier channel.

All model debris flow compositions used monodispersed 3 mm diameter Denstone® 2000 for the coarse granular flow component and water available from the lab (NorPro 2017). The average diameter of the Denstone® 2000 data sheet range, 3.55 mm, was treated as d_{max} for determining the slit barrier ratio (NorPro 2017). Tests termed 'viscous' debris flows had 5 % of the Denstone® 2000 mass replaced with the equivalent mass of dry powdered kaolin. Gravimetric water content was set at 45 % and remained constant for all tests. Table 2 states the exact values used in each composition. Coarse grains and water or pre-mixed suspension were combined in the hopper and stirred continuously to prevent segregation prior to release (Bowman & Sanvitale 2009). Model samples were released via a gate in the hopper base controlled by a pneumatic switch.

Table 2. Viscous (K5) and non-viscous (NV) sample components.

Test Code	Denstone® 2000 Mass (g)	Kaolin Mass (g)	Water Content
NV	2222	0	0.45
K5	2111	111	0.45

Three channel configurations of the flume were used, with a viscous (K5) and non-viscous (NV) interstitial fluid tested in each case. These included: No Barrier (NB) and with slit barriers of ratios 2.3 (2.3B) and 3.6 (3.6B). Slit barriers were placed 550 mm from the flume origin as shown in Figure 4 and are made of acrylic with dimensions shown in Figure 4.

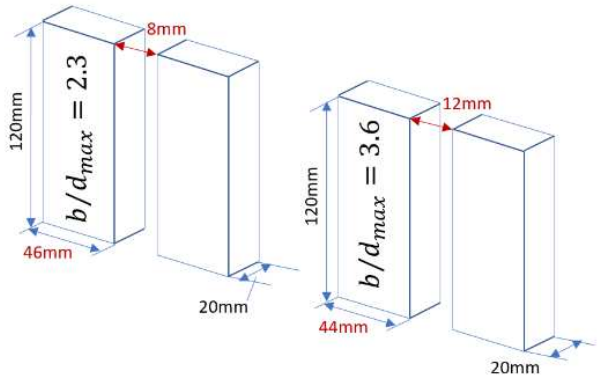

Figure 3. Slit barrier dimensions.

Depositional profile heights and final runout lengths were measured at 10 mm increments of the deposit. Flow velocities were calculated using time difference between the start of flow readings on load cells 1 and 2, as acceleration is assumed negligible over 263 mm gap between sensors. Times were verified using high speed images taken through sidewalls. Flow height postprocessing used lowpassIIR filloutlier functions.

3 RESULTS & ANALYSIS

3.1 Rheology of kaolin suspension

Figure 5 shows the dynamic viscosity outputs plotted on a log scale with increasing shear rate for all three trials per sample in both volume sizes. Data has been presented as in the style of existing literature by Kameda & Morisaki (2022), with standard water viscosity value for reference. The kaolin suspensions demonstrate a non-Newtonian shear-thinning behaviour. The results are consistent with existing rheometric studies of clay suspensions.

Data variation is limited between readings, showing the behaviours observed to be largely unaffected by scaling. This confirms the appropriate use of the equipment specified rpm conversion factor for both volumes and suitable application of suspension behaviour to larger debris flow samples being used in the flume apparatus (elcometer® 2007). The small variation in samples is assumed to be from a contact change between the TL5 bulb and the suspension, with more fluid to mobilise in the larger volume.

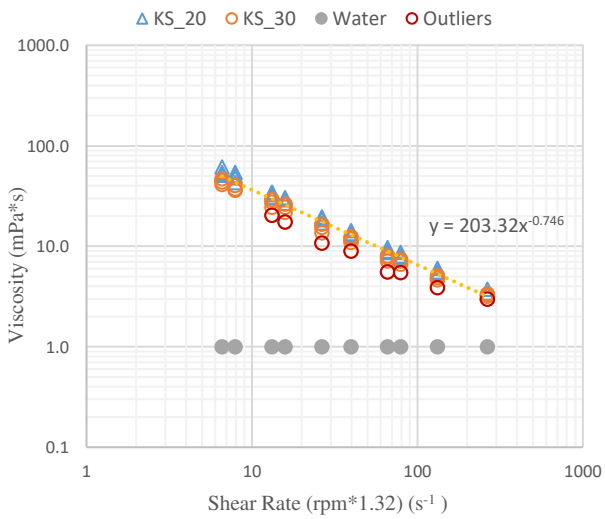

Figure 5. Non-Newtonian behaviour of kaolin suspensions.

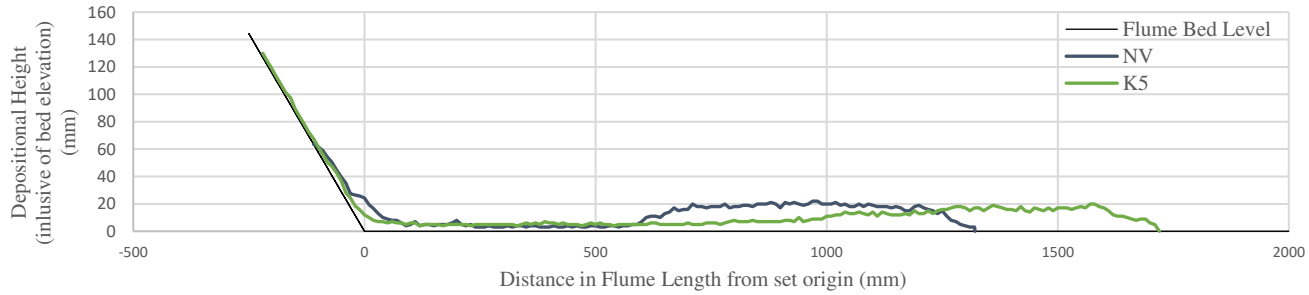

Figure 6. Depositional profiles of viscous (K5) and non-viscous (NV) model debris flow samples.

3.2 Unobstructed flume experiments

3.2.1 Depositional profiles & runout lengths

Figure 6 shows the deposit profiles left by the arrested sample in the flume channel. The presence of kaolin in the interstitial fluid both increases the runout length by 30 % and decreases the average main surge deposit height by 11 % compared to the control NV sample. This is also accompanied by a change in depositional profile shape. The K5 profile shows a smooth gradient up to maximum height of the main surge deposit ('lobe') compared to the sudden, almost step change, observed in the NV sample. This suggests a different distribution of coarse grains in the sample during flow. Observation of the high speed images of flow show an apparent smaller dry granular front for KV samples, however it is easier to see the kaolin suspension interstitial fluid from its opaque nature. Data trend directions are consistent with results presented by de Haas et. al. (2015) and agrees with observations by Kaitna et. al. (2016) for a reduced phase segregation.

3.2.2 Flow velocities

Table 3 shows the calculated and output PIV values for the basal flow velocities.

Table 3. Flow heights and basal velocities.

Test Code	Peak Flow Height (mm)	Velocity (m/s)	PIV Basal Velocity (m/s)
NV_NB	18.77	1.41	1.38
NV_2.3B	18.45	1.46	-
NV_3.6B	18.52	1.48	-
K5_NB	21.56	1.70	1.75
K5_2.3B	*Random spike error*	1.72	-
K5_3.6B	20.30	1.61	-

Viscous flows containing kaolin in suspension consistently have higher basal velocities (1.68 m/s average) compared to the non-viscous interstitial fluid counterpart (1.45 m/s average). This is a 15 % increase for averaged values across tests and a 27 % increase between PIV basal velocity outputs. The faster velocities of viscous flows is consistent and percentage change close to measurements found by de Haas et.al. (2015).

3.3 Slit barrier experiments

3.3.1 Flow-barrier interactions in motion

Figures 7 & 8 show the interaction process between incoming flow and installed slit barrier, 2.3B and 3.6B respectively, over the test duration. Photos have been selected at key behaviour attributes and compared at near equivalent time for the control NV flow composition.

Both K5 and NV flows accumulate a deposited region of grains in a triangle at the base of the slit barrier (the dead zone, 'DZ'). However, as more incoming material reaches the barrier and DZ, K5 compositions develop a steeper zone which reaches further up the barriers. In tests with 3.6B, the arrival of the oversaturated main flow body at the dead zone face almost leads to overtopping when a sudden surge up the barrier face is observed in the video footage. This zone later expands into a rectangular shape as more grains are deposited, whereas the DZ of both NV samples remains mostly in a triangular form. The rectangular dead zone also appears to be held briefly as an upright vertical face as flow travels vertically upwards before backflow occurs.

By application of findings in Section 3.2, this change is found likely to be due to the more energetic viscous flows requiring higher levels of fictional loss before deposition of flow can occur. For example, the incoming flow is able to travel over stationary material for a longer period with fewer grains being deposited at the base region of the dead zone as seen in Figure 7 & 8. In the case of the 3.6B a smaller surface area will

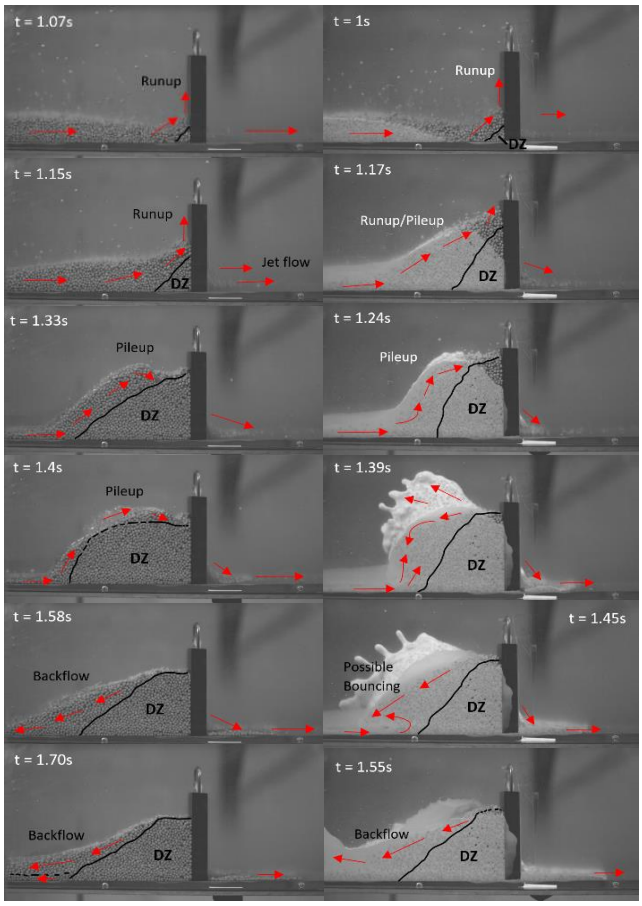

Figure 7. Barrier-flow interaction over time, presented in style of Zhou et.al. (2019), for a 2.3 slit ratio. Left – control NV test. Right- viscous K5 test.

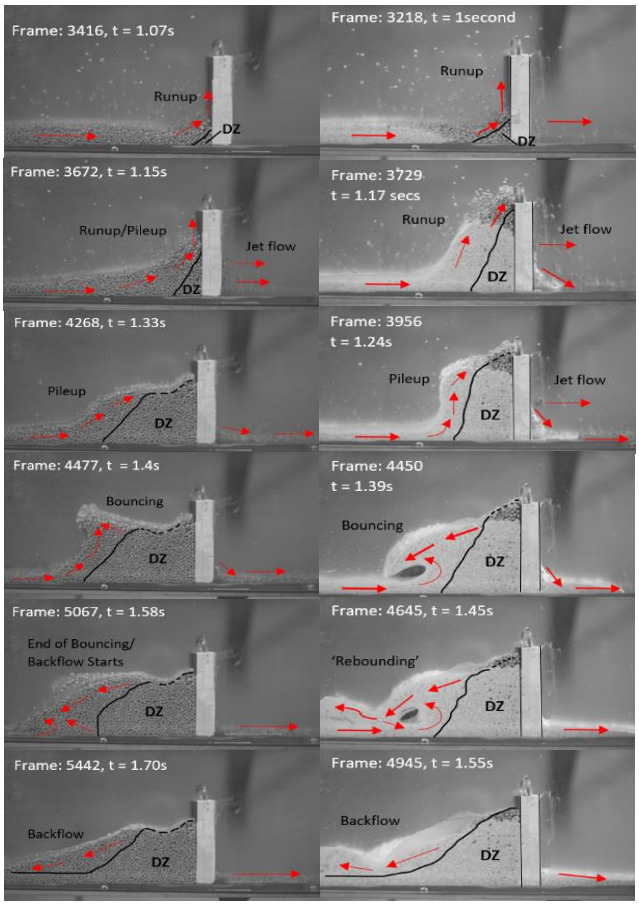

Figure 8. Barrier-flow interaction over time, presented in style of Zhou et.al. (2019), for a 3.6 slit ratio. Left – control NV test. Right- viscous K5 test..

reduce the level of energy dissipated leading to a flow bouncing phenomena, seen in existing research and in control tests in Figure 8 (Zhou et.al. 2019). The viscous case, K5, also presents a bouncing behaviour, however the bouncing crest is observed to extend into a wave formation which is held in position away from the main flow body until it strikes the remaining incoming fluidised tail, as seen at t=3.9 to 4.5 s in Figure 8. Limited mixing is also noticed between the wave and incoming flow, producing a more obvious 'rebounding' of the wave off the still arriving material in the K5_3.6B case which is not seen in the NV_3.6B test. Similar interactions in the K5_2.3B case are seen during maintenance of two different flow directions compared to the NV_2.3B trial. This is potentially from the non-Newtonian aspects of kaolin suspensions leading to changes in viscosity as the shear rate changes due to interaction with the barrier in different locations. However, more data is required to attribute these phenomena to the suspension rheological properties and is an area for further research.

Overall, the K5 flows appears to amplify some features of a NV flow interaction, such as potential bouncing unusually seen in the smaller slit size for K5 barrier tests and observed higher runup heights shown in Figures 7 & 8, while also displaying some new features such as 'rebounding'.

3.3.2 Barrier efficiency and pile up heights

Barrier pile up height and trapping efficiency showed negligible differences (below 10% change) for both comparison between slit sizes used and NV and K5 sample compositions. This is likely to be due to the small 4mm increase from the 2.3B to the 3.6B slit sizes. However, a change in the dead zone gradient was still apparent in depositional profiles.

4 CONCLUSIONS

This study presents preliminary findings for the variation of viscosity in granular debris flows caused by the suspension of clay particles in the interstitial fluid using a small scale flume. Key findings and observations include:

- Kaolin suspensions exhibit a non-Newtonian rheology and are shear-thinning.
- Viscous granular samples return longer runouts, higher velocities, altered depositional profiles and more energetic responses to a slit barrier channel obstruction compared to a pure water interstitial fluid.

Overall, results suggest the lubrication of coarse grains with a viscous fluid allows levels of kinetic energy to be maintained while adding some frictional resistance between phases decreasing segegation. Further research is required to confirm observations and assess the sensitivity of findings.

5 ACKNOWLEDGEMENTS

Thanks to M. Foster for all technical support provided for the duration of this project and to C. Holland for provision and aiding setup of the viscometer apparatus.

Funding provided by UKRI EPRSC has enabled the write up of this work and progression of the first author to a PhD study.

6 REFERENCES

Bowman, E. T. and Sanvitale, N. (2009) 'The role of particle size in the flow behaviour of saturated granular materials', in *Proceedings of the 17th International Conference on Soil Mechanics and Geotechnical Engineering: The Academia and Practice of Geotechnical Engineering*, pp. 470–473. doi: 10.3233/978-1-60750-031-5-470

Cabrera, M. *et al.* (2018) 'Effects of viscosity in granular flows simulated in a centrifugal acceleration field', in *Proceedings of the 9th International Conference on Physical Modelling in Geotechnics.* London, July 2018, London: CRC, pp. 1075-1080

Choi, C. E. *et al.* (2016) 'Coarse granular flow interaction with slit structures', *Geotechnique Letters*, 4(6), pp. 267–274. doi: 10.1680/jgele.16.00103

Coussot, P. and Ancey, C. (1999) *Rheophysical classification of concentrated suspensions and granular pastes*. doi: 10.1103/PhysRevE.59.4445

De Haas, T. *et al.* (2015) 'Effects of debris flow composition on runout, depositional mechanisms, and deposit morphology in laboratory experiments', *Journal of Geophysical Research: Earth Surface*, 120(9), pp. 1949–1972. doi: 10.1002/2015JF003525

elcometer® (2007) *Elcometer 2300 Rotational Viscometer and ViscosityMaster Software Operating Instructions*. Available at: www.manualslib.com/manual/1594868/Elcometer-2300-Series.html?page=2#manual (Accessed: 18 January 2024).

Hu, H. *et al.* (2020) 'Effect of slit size on the impact load against debris-flow mitigation dams', *Engineering Geology*, 274. doi: 10.1016/j.enggeo.2020.105764

Iverson, R. M. (1997) 'The physics of debris flows', *Reviews of Geophysics*, 35(3), pp. 245–296. doi: 10.1029/97RG00426

Kaitna, R. *et al.* (2016) 'Effects of coarse grain size distribution and fine particle content on pore fluid pressure and shear behaviour in experimental debris flows', *Journal of Geophysical Research: Earth Surface*, 121(2), pp. 415–441. doi: 10.1002/2015JF003725

Kameda, J. and Morisaki, T. (2022) 'Rheological properties of concentrated allophane, halloysite, and kaolinite suspensions', *Applied Clay Science*, 226. doi: 10.1016/j.clay.2022.106557.

Michaels, A. S. and Bolger, J. C. (1962) *THE PLASTIC FLOW BEHAVIOR OF FLOCCULATED KAOLIN SUSPENSIONS*. UTC. doi: 10.1021/i160003a001

Nguyen, V. B. Q., Kang, H. S. and Kim, Y. T. (2018) 'Effect of clay fraction and water content on rheological properties of sand–clay mixtures', *Environmental Earth Sciences*, 77(16). doi: 10.1007/s12665-018-7748-0

Nichols H. (2023) *Investigation into the impact of percentage clay content in debris flows on slit barrier design.* MEng Dissertation. University of Sheffield.

NorPro, S.-G. (2017) *Denstone® 2000 Support Balls Supreme Reliability and Survival from Denstone®*. Available at: www.norpro.saint-gobain.com/sites/hps-mac3-cma-norpro/files/2021-06/sgnorpro-denstone-2000-support-media_0.pdf

Turnbull, B., Bowman, E. T. and McElwaine, J. N. (2015) 'Debris flows: Experiments and modelling', *Comptes Rendus Physique*. Elsevier Masson SAS, pp. 86–96. doi: 10.1016/j.crhy.2014.11.006.

Van Olphen, H. (1977) *An Introduction to Clay Colloid Chemistry.* 2nd edn. USA: Wiley-Interscience. ISBN: 0-47-01463-X

Vandine, D. F. (1996) *Debris Flow Control Structures for Forest Engineering*. Available at: www.for.gov.bc.ca/hfd/pubs/Docs/Wp/Wp22.htm (Accessed: 26 May 2023).

Winter, M. G. (2019) 'Landslide hazards and risks to road users, road infrastructure and socio-economic activity', in *17th European Conference on Soil Mechanics and Geotechnical Engineering, ECSMGE 2019 - Proceedings*. International Society for Soil Mechanics and Geotechnical Engineering, pp. 196–228. doi: 10.32075/17ECSMGE-2019-1118

Zhao, Y. *et al.* (2024) 'Fluid effects in model granular flows', Granular Matter, 26(1). doi: 10.1007/s10035-023-01365-4

Zhou G.G.D. *et. al.* (2019a) 'Depositional mechanisms and morphology of debris flow: physical modelling', Landslides, 16, Pp. 315-332, doi: 10.1007/s10346-018-1095-9

Zhou, G. G. D. *et al.* (2019) 'Experimental study on the regulation function of slit dam against debris flows', *Landslides*, 16(1), pp. 75–90. doi: 10.1007/s10346-018-1065-2.